RSC Advances

PAPER

View Article Online
View Journal | View Issue

Cite this: *RSC Adv.*, 2025, **15**, 28959

Antihyperglycemic drug screening: 4-nitrophenol intermittent pulse amperometry as a convenient α-glucosidase inhibitor assay

Waswan Prempinij and Albert Schulte *

We present intermittent pulse amperometry (IPA) as a practical direct electrochemical readout option in a 4-nitrophenol (4-NP)-assisted α-glucosidase (α-GL) activity assay. The feasibility of the strategy was validated through proof-of-principle inhibition tests on a selection of gold-standard α-GL inhibitors and commercial inhibitor-containing plant-based food supplements, and the quality of the obtained results confirmed well the potential of this method in the identification of new antidiabetic drugs. The proposed IPA/4-NP-based α-GL activity inhibition assay is an easy-to-establish user-friendly approach for the rapid and economical detection of inhibitor candidates within small to medium-sized sample libraries and is intended to complement, not replace, other currently used methods and to valuably widen the analytical scheme set for applicants in the academic and industrial pharma sectors.

Received 31st May 2025
Accepted 1st August 2025

DOI: 10.1039/d5ra03861h

rsc.li/rsc-advances

1. Introduction

Diabetes mellitus is a huge problem worldwide, and the number of cases of this chronic disorder is high and constantly rising. The causes of *diabetes mellitus* are defects in insulin secretion and sensitivity, leading to hyperglycaemia, a rise of the blood glucose concentration to harmful levels.[1] α-glucosidase (α-GL) inhibitors, which slow down intestinal polysaccharide digestion and delay blood glucose absorption, are active components of feasible oral antihyperglycemic medications.[2,3]

Known α-GL inhibitors include natural and synthetic organic chemicals, and the search for new drugs needs analytical tools for candidate library screening.[4] In current routine use are optical inhibitory assays with 4-nitrophenyl-α-D-glucopyranoside (4-NP-G) as a synthetic α-GL substrate, the product of α-GL-catalysed 4-NP-G hydrolysis, 4-nitrophenol (4-NP), being determined spectroscopically from its absorbance at 400 nm.[5] An optical 4-NP assay readout has the drawbacks that, for instance, the 4-NP colour creation requires a change of the assay buffer pH to strongly alkaline; real-time enzyme activity monitoring is thus not possible, the method is time-consuming, and testing in samples with inherent colour or turbidity is hard. To overcome these limits, electrochemical (EC) 4-NP testing has recently been suggested as a substitute, owing to the advantages of an EC detection with modern potentiostat equipment.[6–8] As in an optical α-GL assay, the rate of enzyme-catalysed 4-NP release is determined as a measure of α-GL activity but *via* anodic analyte oxidation at solid electrodes, instead of by photometry. A known drawback of anodic 4-NP detection is, however, that the process creates phenoxy radicals that may couple and form a polymer film on the electrode.[9] This "surface fouling" depends on electrode potential, electrolyte, and temperature and the gradual formation of a polymer film on the electrode surface, from recombination of phenoxy-radical intermediates finally leads to poor signalling. Work with fouling-resistant boron-doped diamond (BDD) electrodes, use of protective electrode coatings, running electrode reactivation steps within measurement sequences and work with fouling inhibitors were previously proposed as tactics to overcome sensor fouling.[10] As a much easier anti-fouling option, we recently reported intermittent pulse amperometry (IPA), which allowed reliable 4-NP detection with insignificant signal disturbance and a 10 μM practical limit of detection, without sensor premodification or the use of complex detection methods.[11] It was also shown that IPA was practicable for monitoring the action of *N*-acetyl-β-D-glucosaminidase on 4-NP-labelled *N*-acetyl-β-D-glucosamine. Worth mentioning that the pulsed IPA-based amperometric detection offers a key advantage over differential pulse (DPV) and linear sweep voltammetry (LSV) and constant potential amperometry (CPA): the working electrode (WE) is in IPA mode only for about half a second per data point at the phenol oxidation potential. This short exposure reduces the risk of electrode fouling from phenol radical recombination and polymer film formation. In contrast, DPV, LSV and CPA expose the WE to high anodic potentials longer, increasing the likelihood of phenol polymerization, fouling, and signal decline.

New potent α-GL inhibitors, certainly those originating from natural sources, are key targets in therapeutic diabetes management and diabetes-related syndromes and are needed

School of Biomolecular Science and Engineering, Vidyasirimedhi Institute of Science and Technology (VISTEC), Wang Chan Valley, Rayong 21210, Thailand. E-mail: albert.s@vistec.ac.th; Tel: 0066 (0) 873 758 518

to improve public health outcomes. To support the search for novel drugs, we propose here an IPA-based electrochemical 4-NP detection as an alternative simple α-GL activity assay and a convenient method for α-GL inhibitor identification.

2. Experimental section

Main study enzyme was a rice α-GL (type V, ammonium sulphate suspension, 40–80 units per mg protein, Sigma-Aldrich. CAS NO. 9001-42-7) and the test solutions and samples for rice α-GL inhibition trials were prepared in 0.1 M acetate buffer, pH 4.0, which was the optimal pH for this protein. Best electrolyte for work with a yeast α-GL *Saccharomyces cerevisiae* (type I, lyophilized powder, Sigma-Aldrich. CAS no. 9001-42-7) was a phosphate buffer of pH 7.0. All trials were done in a 5 mL beaker-type EC cell with a three-electrode system, including a platinum (Pt) wire counter-electrode (CE) and a commercial Ag/AgCl (3 M KCl) reference-electrode (RE). WE choice was because of its literature-known wide potential window and resistance to sensor surface fouling a disc-shaped commercial boron-doped diamond (BDD) electrode of 3 mm diameter and thus a geometric area of about 0.071 cm^2.[12–14] Though they were not used in this study, nowadays available screen-printed BDD electrode platforms are recommended as practicable and cheap WE alternative.

The detection and resting potentials for the IPA of the rice and yeast α-GL assays were selected from the 4-NP cyclic voltammograms in the assay buffer (Fig. S1 and S7, SI) and set to the values of the 4-NP peak response (+1.065 V per rice; 0.95 V per yeast) and zero current (0.0 V), respectively. Details of the IPA data acquisition and analysis are listed in the SI. For trials in the rice α-GL assay buffer of this study Fig. 1 compares anodic 4-NP IPA with 4-NP CPA. As in the earlier IPA study, the pulsed scheme provided a stable anodic readout, while the use of CPA suffered from the decline of the signal to almost zero. Details of the chemicals, the equipment, and the electrochemical IPA-based 4-NP detection are listed in the SI.

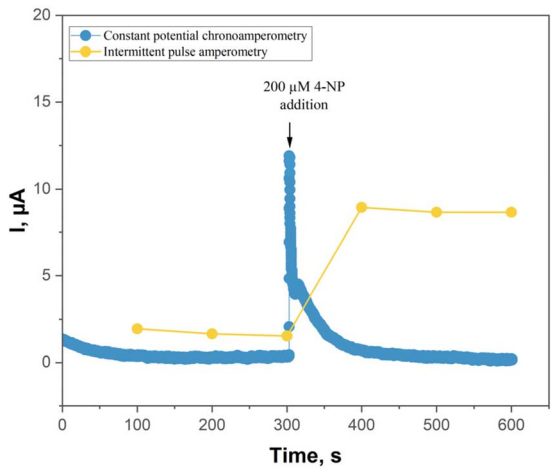

Fig. 1 Amperometric trace of a 200 μM increase in 4-NP concentration in 0.1 M acetate buffer, pH 4.0 by constant potential amperometry at +1.065 V (blue) and intermittent pulse amperometry (IPA) with 0.5 detection pulses applied every 99.5 s (yellow).

3. Results and discussions

3.1. 4-NP IPA: method performance test

Please note that the reducible nitro group is present in both free 4-NP and the 4-NP-G substrate, but the phenol's hydroxyl group in 4-NP-G is bonded to the sugar entity, obstructing the electrooxidation. Therefore, our enzyme activity assay tackled the oxidation of the phenol's hydroxyl group, while the cathodic reduction of the nitro group was not a readout option. Before the 4-NP IPA assay was used to measure inhibition of rice α-GL, the validity of the previously reported response linearity, analyte sensitivity and analyte recovery rate performance were checked in triplicate repetitions. The data points for six increasing 4-NP concentrations between 50 and 500 μM were linearly aligned (Fig. S2A (SI)) with a regression line gradient (=sensitivity) of 30.3 nA μM^{-1}, which was of the same order of magnitude. Quantification of the 4-NP content of a 100 μM model sample was also performed, with 106.9 ± 1.7% (n = 3) recovery from standard addition plot analysis (Fig. S2B (SI)) verifying the ability of IPA to quantify 4-NP. The use of 4-NP IPA as a possible α-GL activity assay was next assessed.

3.2. 4-NP IPA: use as rice α-GL inhibition assay

In initial trials the inhibition of rice α-GL was assessed with the 4NP IPA-based assay for the interaction of the enzyme with the known inhibitors acarbose,[15] miglitol[16] and voglibose.[17] Routinely, rice α-GL in 0.1 M acetate buffer, pH 4.0 was hatched at 37 °C with or without (control) the presence of inhibitor. Pre-incubated mixtures were loaded into a ready three-electrode EC cell and after 4-NP-G addition the reaction rate was measured by IPA at room temperature. Repeated assay test runs suggested 0.5 s-long increases to +1.065 V and rests for 299.5 s at 0.0 V, 79.0 U L^{-1} α-GL, 1 mM 4-NP-G and 30 min as best IPA parameters, rice α-GL concentration, substrate concentration and preincubation time, respectively (Fig. S3 and S4 (SI)).

The sketch in Fig. 2 shows the basic principle of the electrochemical α-GL inhibitory assay with IPA-based readout of 4-NP product formation. For sample loads with or without inhibitor baseline IPA data were acquired for 10 min, 1 mM 4-NP-G substrate was then added, and the IPA current recording was continued for 30 min. A typical IPA-based assay recording of α-GL activity is shown in Fig. S5 (SI). Visible is the current response to a series of eight detection pulses, all of which appear as upright lines with 5 dots. The Fig. inset is a zoom of one dot set and obvious are the 5 current values that are stored while a 500 ms detection pulse is applied to the WE. The capacitive charging current contribution to the signal is high for data point 1 but decays exponentially and is negligible for data point 5. The EC α-GL inhibition profiles in Fig. 3 and 4 hence show the means of data point 5 current readings from triplicate trial repetitions, while those for data points 1–4 were omitted.

Fig. 3A shows five electrochemically completed α-GL inhibition profiles for serial dilutions of the inhibitor acarbose,

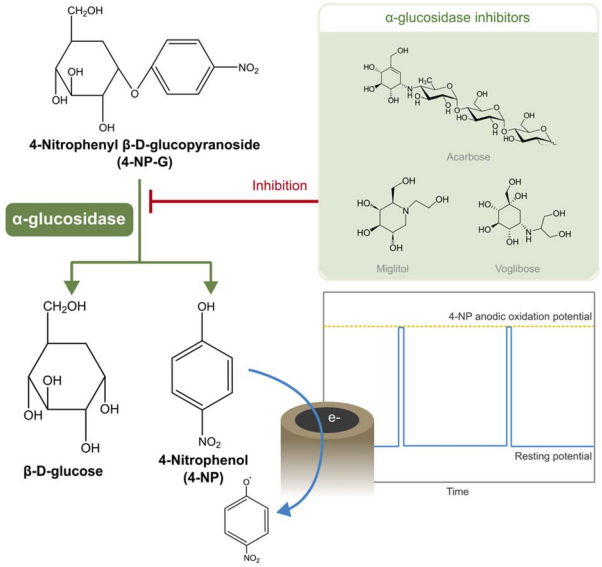

Fig. 2 Chemical structures of the α-GL inhibitors acarbose, miglitol and voglibose (right) and the redox-labelled α-GL substrate 4-nitrophenyl-β-glucopyranoside (4-NP-G, left). α-GL acts on the substrate 4-NP-G and converting it into sugar and electroactive 4-NP, which is detected on a boron-doped diamond working electrode by amperometry in the intermittent pulse mode. The concentration of 4-NP detected is directly related to α-glucosidase activity and thus measures the effectiveness of potential inhibitors.

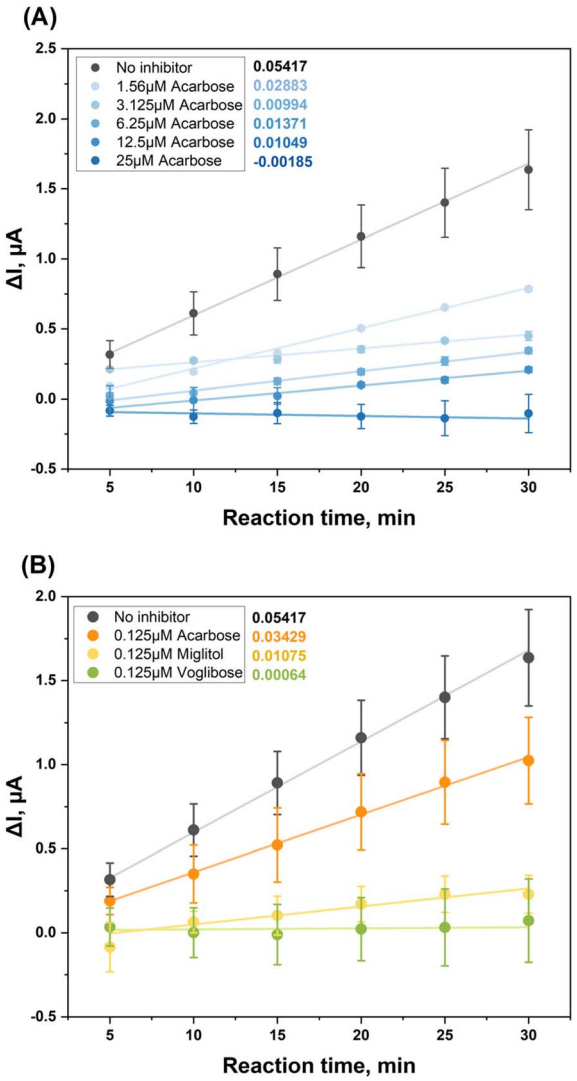

Fig. 3 Anodic 4-NP/IPA-based α-GL inhibition profiles for (A) the concentration-dependent acarbose inhibition at 0 (black), 1.56, 3.125, 6.25, 12.5 and 25 μM (shades of blue) and (B) comparison of the inhibition by three different α-GL inhibitors at equal concentrations (0.125 μM): acarbose (orange), miglitol (yellow) and voglibose (green), no inhibitor (black). Curve slopes are listed in μA min^{-1} along with the data labels. Data points are means of triplicate repetitions and errors bars are standard deviations. Slightly negative Δ*I* values in (A), for high acarbose levels and short reaction times and in (B) for miglitol and voglibose are caused by a gradual drift of background reactions due to electrode surface oxidation and/or residual oxidizable electrolyte content other than 4NP toward lower levels over time.

from 25 to 1.56 μM, with uninhibited α-GL included as a control. The trend lines through data points reflect the gradual increases in 4-NP concentration in the cell produced by the hydrolytic activity of α-GL with the substrate 4-NP-G. A greater line slope corresponds to greater α-GL activity. As expected, an increase in the concentration of the α-GL inhibitor acarbose led to lower enzymatic activity and a corresponding decline in the curve gradient. Fig. 3B compares the IPA-based α-GL activity profiles on exposure to three different known α-GL inhibitors at the same 0.125 μM concentration, for data from triplicate trial repetitions. Even at nanomolar levels, acarbose, miglitol and voglibose suppressed the hydrolytic activity of α-GL on 4-NP-G by about 37, 80 and 99%, respectively and their relative potencies were accurately reflected, aligning with published data. Acarbose was correctly identified as the weakest inhibitor, miglitol exhibited intermediate activity, and voglibose was the most potent α-GL effector.[18] Reported IC50 values for these compounds vary depending on assay conditions and data sources; direct comparisons within a single assay were not found. Nevertheless, our electrochemical assay with pulsed amperometry for released 4-NP detection successfully detected inhibition at levels far below the known micromolar IC50 ranges, demonstrating its sensitivity and effectiveness.

The 30-min-long α-GL inhibition tests of Fig. 3 and 4 used freshly polished BDD disc electrodes with a clean surface and the achievement of reliable data suggested that the response consistency and stability of the applied IPA readout was well suitable to reach trustful information about the enzyme activity in inhibitor presence or absence. After completion of an electrochemical enzyme inhibition trial, the used BDD electrode was cleaned and regenerated through a gentle repolishing on an alumina-soaked polishing pad, enabling an unlimited reuse for the detection 4-NP release in the α-GL activity assay.

3.3. 4-NP IPA: use for antihyperglycemic drug screening

A variety of herbal antidiabetics are available in drugstores in tablet form. Effective pill factors are natural α-GL inhibitors that delay the digestion of carbohydrates and reduce the

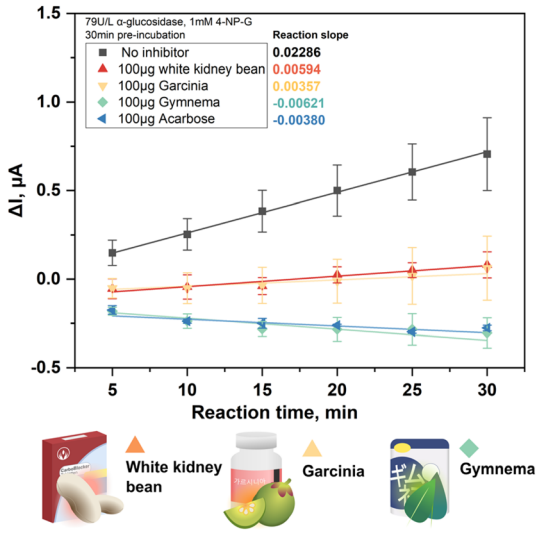

Fig. 4 Application of the 4NP-assisted electrochemical α-GL assay to testing the effect on α-GL of three antidiabetic supplements with claimed active ingredients. Comparison of changes in 4-NP IPA currents (concentrations) for the trial with no inhibitor exposure (black, control), and for the inhibition trials with extracts of white kidney bean (*Phaseolus vulgaris*, orange), *Garcinia cambogia* (yellow) and *Gymnema silvestre* (green), with acarbose as a positive control (blue). In each case 100 mg of the preparation was added to the solution with the glucosidase. Data points are the means of the results of triplicate trial repetitions and errors bars are standard deviations. The values of the line slopes (=rates of enzyme reaction) in each case are marked next to the data labels. For explanations of the appearance of negative *y*-axes values refer to the legend of Fig. 3.

postprandial blood glucose level. A good means of proving the applicability of the IPA-based assay of this study as a practical tool for α-GL inhibitor screening was thus a check of the α-GL inhibition potency of three randomly chosen commercial antidiabetic supplements. The three plant-derived formulations came from Germany, Japan and South Korea and had as functional factors extracts of white kidney beans (*Phaseolus vulgaris*)[19] and the herbs *Gymnema* (*Gymnema sylvestre*)[20] and Garcinia cambogia ('*Malabar tamarind*'),[21] respectively. Acarbose was used as a positive control while α-GL activity measurements in the absence of any inhibitor species served as a negative control.

Details of the individual sample preparations are given in Fig. S6 (SI). Briefly, tablets of the herbal formulations were first pulverized into fine powders, 100 mg of which were combined with 1 mL de-ionized (DI) water. Each mixture was thoroughly stirred, the resulting aqueous suspensions centrifuged to remove insoluble components, and the clear supernatants were used as stock solutions. For acarbose the treatment of 100 mg of the water-soluble powder was identical but the centrifugation step was omitted. The test sequence for the demonstration of the inhibitor activity was that already used successfully for the three organic substances with proven pharmacologic effect, namely acarbose, miglitol and voglibose. In each case 30 µL of 10× dilutions of the 100 mg aqueous supplement extractions (or 30 µL of the 10× dilution of the aqueous acarbose stock solution) were added to 2970 µL test buffer with 79 mU mL^{-1} α-GL. The mixture obtained was pre-incubated at 37 °C for 30 minutes and then put in the electrochemical cell with the counter, reference and working electrodes and a stir bar. After 10 minutes of baseline recording in gently stirred solution, the α-GL substrate, 4-NP-G, was added to a final concentration of 1 mM and biocatalytic 4-NP release was followed at room temperature by the electrochemical IPA assay. Data from triplicate test repetitions of each case are shown in Fig. 4.

As in the drug test shown in Fig. 3, the slopes of regression lines through plots of 4NP oxidation current/reaction time reflect the rate of change of the concentration of free 4-NP and thus are measures of α-GL activity. Simple comparison of the acquired curve slopes revealed that the *Gymnema* supplement was as good an α-GL inhibitor as the anti-diabetic drug factor acarbose; at the chosen test dose both agents were able to suppress the α-GL activity fully. On the other hand, the kidney bean and tamarind extracts, used at the same dose, produced smaller but still significant inhibitions. The % inhibition for the runs in inhibitor absence (control) and with kidney bean, tamarind and *Gymnema* extracts and acarbose present were 0, 74, 84, 100 and 100, respectively ($n = 3$).

3.4. 4-NP IPA: adaptability for different α-GL types

The proposed IPA-aided electrochemical enzyme inhibition assay was not only suitable for rice α-GL, the main study model, but also for α-GL from the yeast, *Saccharomyces cerevisiae*. For the yeast α-GL inhibition test, however, a reaction buffer of neutral pH 7.0 was required for optimal substrate conversion, rather than the slightly acidic pH needed for the rice enzyme. 4-NP cyclic voltammograms in a pH 4.0 acetate and a pH 7.0 phosphate buffer are presented in Fig. S7 (SI). The comparative electrochemical test exposed that slightly different 4NP working electrode (WE) detection potentials had to be chosen for inhibition tests in acetate (for the rice α-glucosidase) and phosphate (for the yeast α-glucosidase) buffer because of a pH-dependent shift in the anodic CV peak potentials of 4NP. Best choice for 4NP detection in acetate buffer of pH 4 was +1.065 V (Fig. S1 and S7) and a slightly less anodic +0.95 V was better for work in phosphate buffer of pH 7 (Fig. S7). The shift of the peak toward more negative values with increasing solution pH suggests that phenol oxidation becomes more favourable at higher pH levels. This is because the 4NP phenol exists in equilibrium with its deprotonated form, the phenolate anion, and the phenolate anion is more easily oxidized than phenol itself.

Further comparative calibration trials with fixed optimal IPA parameter settings confirmed that the adapted pulsed amperometry measured the signalling molecule 4-NP in the relevant concentration range about equally well in acetate buffer, pH 4.0 at +1.065 V and phosphate buffer, pH 7.0 at + 0.95 V (Fig. 5A). With electrochemical 4-NP monitoring in phosphate buffer, pH 7.0, yeast α-GL inhibition by the benchmark inhibitor acarbose was then tested under the similar assay conditions detailed above and in the related the SI section. As good agreement with the performance of the rice α-GL, concentration-dependent inhibition of yeast α-GL by acarbose became evident as a clear

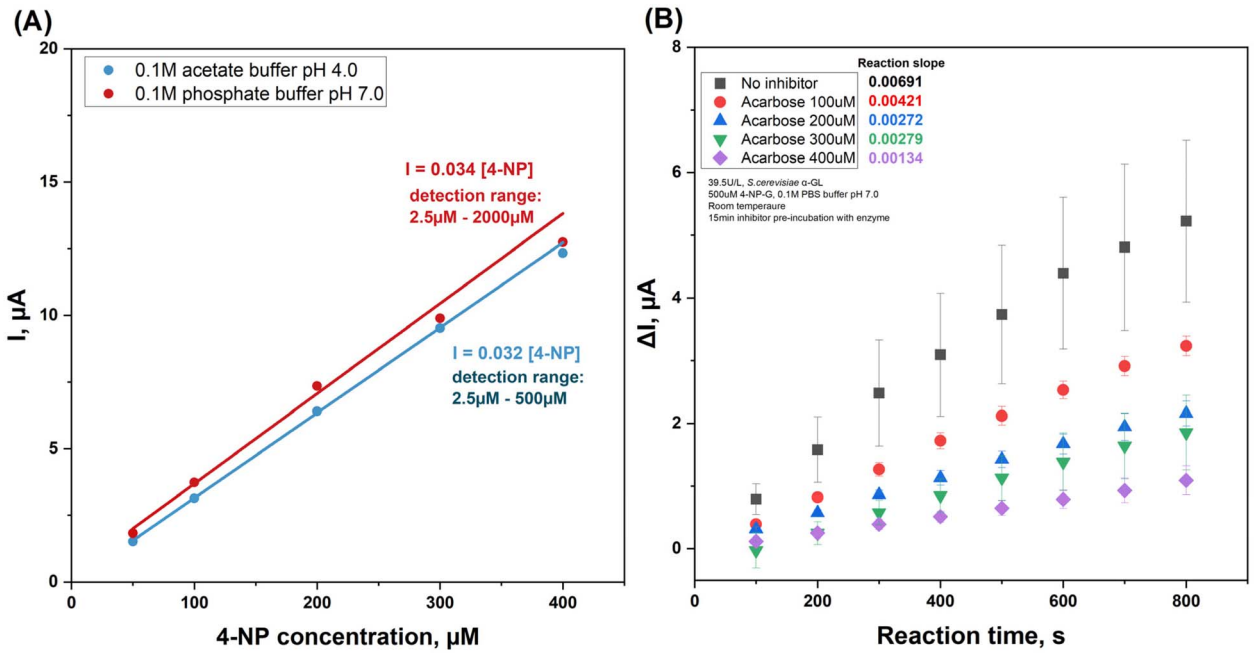

Fig. 5 (A) Comparison of the calibration plots of the 4-NP IPA response in 0.1 M acetate buffer pH 4.0 (blue) and 0.1 M sodium phosphate buffer (Na-PB) pH 7.0. The sensitivity of the 4-NP assay was not dependent on the pH of the assay buffer. (B) Summary of the results of the IPA-based electrochemical yeast α-glucosidase activity assay in the absence (black) and presence of acarbose of various concentrations: 100 µM (red), 200 µM (blue), 300 µM (green) and 400 µM (purple). The assay was carried out as described in the SI, Section 3 and SI Fig. S3.

decrease of the slopes of the acquired 4-NP IPA profiles, indicating decelerated substrate conversion (Fig. 5B) on 4-NP release. That the visualization of inhibitor action with the 4-NP/IPA assay was successful with GLs from both rice and yeast suggests that the strategy is generally applicable as a α-GL inhibitor screen and extension to the wide range of α-GLs from plants, fungi, bacteria, animals and humans is feasible. For successful results with our α-GL assay, it is, however, essential that the pH of the assay test buffer aligns well with the pH optimum of the enzyme model, and that the anodic detection potential for 4NP is adjusted suitably, too.

4. Conclusions

Anodic IPA was shown to be satisfactory and convenient for the detection of α-GL-driven 4-NP release from the substrate 4-NP-G. Inhibition trials with known α-GL inhibitors and with anti-hyperglycemic preparations of plant origin verified the ability of the adapted amperometry scheme to identify inhibition by the compounds tested and to visualize differences in inhibitory potency. An advantage of the proposed EC method for α-GL inhibitor screening is that it succeeds very well with low-cost equipment and in addition is a simple enough in execution to facilitate straightforward identification of potential inhibitor hits. The determination of accurate IC_{50} values is, on the other hand, a challenge for our rapid EC approach, and this task may require standardized sophisticated optical assays. Nevertheless, compared to the recently reviewed more complex optical and EC assay options[22] (refer also to Table S1) the 4-NP-IPA-based assay of this study is a good choice when aiming at a preliminary pre-screening of compound libraries and a classification of individual entries as inactive, weak, or strong inhibitors. And for sample throughput optimization it is feasible to integrate our EC methodology into workstations that are adapted for automated EC measurements. Such own work with the proposed EC α-GL inhibition assay in already established workstations for automated (robotic) execution of electroanalysis and biosensing in microtiter plates[23–26] is envisioned as a strategy to further advance the practicability of α-GL inhibitor screening in collections of organic compounds and plant extracts and to permit labour- and cost-efficient execution of an α-GL inhibitor screening, with a reduced risk of operator errors.

Author contributions

WP: investigation, data curation, formal analysis, methodology, validation, visualization, writing – original draft, writing – review and editing; AS: conceptualization, supervision, resources and project administration, validation, writing – review and editing.

Conflicts of interest

There are no conflicts to declare.

Data availability

The data supporting this article have been included here or as part of the SI.

Supplementary information is available. Included are the details on the used chemicals, materials and instrumentation, the methodology of electrochemical detection of 4-NP, the supplementary Fig. S1–S7 and supplementary Table S1. See DOI: **https://doi.org/10.1039/d5ra03861h**.

Acknowledgements

The authors acknowledge VISTEC support *via* general funding to A. S., a VISTEC PhD scholarship for W. P. and subsidies from the Thailand Science Research and Innovation (TSRI) through Fundamental Funds 2024/2025 to A. S. Dr David Apps, Edinburgh Medical School, Edinburgh, Scotland is thanked for his dedicated manuscript proofreading.

References

1 K. Khunti, Y. V. Chudasama, E. W. Gregg, M. Kamkuemah, S. Misra, J. Suls, N. S. Venkateshmurthy and J. Valabhji, *Diabetes Care*, 2023, **46**, 2092–2101.
2 A. Mushtaq, U. Azam, S. Mehreen and M. Naseer, *Eur. J. Med. Chem.*, 2023, **249**, 115119.
3 S. Kumari, R. Saini, A. Bhatnagar and A. Mishra, *Arch. Physiol. Biochem.*, 2024, **130**, 694–709.
4 G. Pan, Y. Lu, Z. Wei, Y. Li, L. Li and X. Pan, *Heliyon*, 2024, **10**, e37467.
5 X. Zhang, G. Li, D. Wu, Y. Yu, N. Hu, H. Wang, X. Li and Y. Wu, *Food Funct.*, 2020, **11**, 66–82.
6 D. Zhang and Q. Liu, *Biosens. Bioelectron.*, 2016, **75**, 273–284.
7 J. Li, G. He, B. Wang, L. Shi, T. Gao and G. Li, *Anal. Chim. Acta*, 2018, **1026**, 140–146.
8 M. Mohiuddin, D. Arbain, A. K. M. S. Islam, M. S. Ahmad and M. N. Ahmad, *Nanoscale Res. Lett.*, 2016, **11**, 95.
9 T. Yamamoto, T. Saitoh, Y. Einaga and S. Nishiyama, *Chem. Rec.*, 2021, **21**, 2254–2268.
10 B. L. Hanssen, S. Siraj and D. K. Y. Wong, *Rev. Anal. Chem.*, 2016, **35**, 1–28.
11 W. Prempinij, W. Suginta and A. Schulte, *Appl. Phys. Lett.*, 2023, **123**, 033701.
12 Y. Zhou and J. Zhi, *Talanta*, 2009, **79**, 1189–1196.
13 S. J. Cobb, Z. J. Ayres and J. V. Macpherson, *Annu. Rev. Anal. Chem.*, 2018, **11**, 463–484.
14 S. Baluchová, A. Daňhel, H. Dejmková, V. Ostatná, M. Fojta and K. Schwarzová-Pecková, *Anal. Chim. Acta*, 2019, **1077**, 30–66.
15 J.-L. Chiasson, R. G. Josse, R. Gomis, M. Hanefeld, A. Karasik and M. Laakso, *Lancet*, 2002, **359**, 2072–2077.
16 L. J. Scott and C. M. Spencer, *Drugs*, 2000, **59**, 521–549.
17 R. Kawamori, N. Tajima, Y. Iwamoto, A. Kashiwagi, K. Shimamoto and K. Kaku, *Lancet*, 2009, **373**, 1607–1614.
18 K. Tan, C. Tesar, R. Wilton, R. P. Jedrzejczak and A. Joachimiak, *Protein Sci.*, 2018, **27**, 1498–1508.
19 L. Mojica, A. Meyer, M. A. Berhow and E. G. de Mejía, *Food Res. Int.*, 2015, **69**, 38–48.
20 G. Chen and M. Guo, *Front. Pharmacol*, 2017, **8**, 228.
21 P. Shetty, M. Rai, A. Ravindran, H. N. Gopalakrishna, V. R. Pai and B. S. Kalal, *Int. J. Clin. Exp. Pathol.*, 2022, **15**, 380–387.
22 G. Pan, Y. Lu, Z. Wei, Y. Li, L. Li and X. Pan, *Heliyon*, 2024, **10**, e37467.
23 S. Intarakamhang and A. Schulte, *Anal. Chem.*, 2012, **84**, 6767–6774.
24 S. Teanphonkrang and A. Schulte, *Anal. Chem.*, 2017, **89**, 5261–5269.
25 W. Jaikaew, A. Ruff, P. Khunkaewla, T. Erichsen, W. Schuhmann and A. Schulte, *Anal. Chim. Acta*, 2018, **1041**, 33–39.
26 A. Ruff, W. Jaikaew, P. Khunkaewla, W. Schuhmann and A. Schulte, *ChemPlusChem*, 2020, **85**, 627–633.